Biodiversity and thermal ecological function: The influence of freshwater algal diversity on local thermal environments - Submission to ECOLOGY & EVOLUTION

Anouch Missirian[1,*], Eyal G. Frank[2], Jess T. Gersony[3], Jason C. Y. Wong[1], Shahid Naeem[4]

1 School of International and Public Affairs, Columbia University, New York, NY, USA
2 Harris School of Public Policy, University of Chicago, Chicago, IL, USA
3 Department of Organismic and Evolutionary Biology, Harvard University, Cambridge, MA, USA
4 Department of Ecology, Evolution, and Environmental Biology, Columbia University, New York, NY, USA

*** Corresponding author, am4215@columbia.edu**

Abstract

The influence of temperature on diversity and ecosystem functioning is well studied; the converse however, i.e. how biodiversity influences temperature, much less so. We manipulated freshwater algal species diversity in microbial microcosms to uncover how diversity influenced primary production, which is well documented in biodiversity research. We then also explored how visible-spectrum absorbance and the local thermal environment responded to biodiversity change. Variations in the local thermal environment, that is, in the temperature of the immediate surroundings of a community, are known to matter not only for the rate of ecosystem processes, but also for persistence of species assemblages and the very relationship between biodiversity and ecosystem functioning. In our microcosm experiment, we found a significant positive association between algal species richness and primary production, a negative association between primary production and visible-spectrum absorbance, and a positive association between visible-spectrum absorbance and the response of the local thermal environment (i.e., change in thermal infrared emittance over a unit time). These findings support an indirect effect of algal diversity on the local thermal environment pointing to a hitherto unrecognized biodiversity effect in which diversity has a predictable influence on local thermal environments.

Keywords

biodiversity, thermal ecology, ecosystem function, thermography, global change, temperature.

Short title

Biodiversity and thermal ecological function

Introduction

The varied influences of biodiversity on ecosystem functions and properties, and the abiotic components of these systems, are well studied (3, 20, 29). The local thermal environment – most frequently measured as air, water, or soil temperature –, which can be considered an ecosystem-level property, however, has largely been treated as the result of extrinsic or abiotic factors such as climate, special attention being devoted to the impacts of changing temperature on biodiversity and ecosystem properties in the face of recent, unprecedented changes in climate (12). Temperature's effect on ecosystem functioning and biodiversity has been investigated: most notably, the effect of

temperature change on individuals (2), community diversity (18, 26), ecosystem functions (21), but also on many other facets of the ecosystem such as pest dynamics, niche shift, and community turnover, in terrestrial and marine systems alike, as well as the very relationship between biodiversity and ecosystem functioning, e.g., (1, 5, 9, 15, 32, 33)). The influence of biological diversity on temperature, however, is less well studied, despite temperature being an environmental parameter of fundamental ecological importance.

It is important to note that the influence of vegetation type on albedo (e.g., when boreal forest replaces grassland – see for instance (7, 8)) is well studied. However, whether the change in plant species richness shows predictable impacts on albedo is unknown. Our focus, then, is on whether a change in the *diversity* of a given community can affect its thermal properties. Back to the albedo example for instance, whether the change in plant species richness shows predictable impacts on albedo is unknown. So is the broader influence of biodiversity on local thermal environments.

Given the roles biodiversity can play in primary productivity (27) and other ecosystem properties (e.g., stability (10, 17, 28), efficiency (22)), biodiversity effects could translate into a change in the local thermal properties of the system, though the direction and magnitude are difficult to predict. Indeed, in terrestrial systems for example, if more diverse communities had higher albedo or greater evapotranspiration associated with greater production, the local temperature could decrease. On the other hand, local temperature could just as well decrease in more diverse communities if increasing diversity led to increasing dominance by darker plants, hence to increased absorbance, leading to visible spectrum radiation being re-emitted as thermal radiation. Germanely, diversity could have either or both of these countervailing effects in aquatic systems: increasing temperature by increasing productivity, decreasing temperature by increasing efficiency, on top of community albedo effects.

To explore this issue, we manipulated algal biodiversity in freshwater microcosms to test for diversity effects on local thermal environments; microcosm refers to the closed system in its entirety, i.e. culture vessels with their culture medium and phytoplankton community. Algal species are key members of aquatic communities that are concentrated in upper surfaces of the water column where light is abundant. They play a key role in aquatic environments as primary producers, and in global biogeochemical cycles; yet little is known of their patterns of diversity (see (13)) and how they relate to primary production (see (30)). Because planktonic algal species contain a variety of pigments (4, 11), they absorb visible spectrum light (0.40 – 0.90 μm), some of which is used for photosynthesis, but a large portion of the remainder is re-emitted as thermal infrared (7.5 – 13.0 μm), which produces sensible heat that warms the water around them. Global changes are affecting freshwater and marine communities and their diversity (24), and therefore make algal communities of additional interest from an environmental perspective. While the impacts of temperature change on algal communities, or indeed any biological community, are important as climate change increases, the role biological communities play in their changing thermal environments is unknown and could be important for understanding more clearly the two-way interaction between temperature and ecosystems.

Materials and Methods

We used a microcosm setup for maximal control over the variables of interest, our objective being to observe whether or not community diversity, more precisely here, species richness, has an effect on the local thermal properties of ecosystems. Thus our focus is not on productivity (or its proxies, such as Chlorophyll a or greenness): the relationship between producer diversity and production has been well studied. Rather, we focus on the effect of species richness on the radiation of thermal infrared (sensible heat) resulting from the absorption of visible light. We chose species richness as a measure of diversity to minimize the numbers of degrees of freedom and the magnitude of this novel experiment, and also to conform to the long tradition of experiments in biodiversity and ecosystem functioning (19, 27) and thus make ours comparable to that rich body of literature. We measured sensible heat using thermography. Thermography quantifies thermal infrared radiation, in particular that emitted by the focal organism(s) (e.g., mammals, molluscs (14, 25), or here, phytoplankton); it is distinct from greenness, which concerns reflected light (most often from chlorophyll in relatively transparent freshwater algal species).

We used algae as a model group. The algae communities consisted of 0 (control), 1, 2, 4, or 8 species drawn from a pool of eight species. These were: *Ankistrodesmus falcatus*, *Chlamydomonas reinhardtii*, *Chlorella vulgaris*, *Cosmarium turpinii*, *Eudorina elegans*, *Haematococcus droebakensis*, *Selenastrum capricornutum*, *Staurastrum gracile*. All species are freshwater algae that are commonly found in lakes and other water bodies under temperate

climates, with standard nutrient and growth medium requirements (e.g., none uses silicon, and all grow at ambient temperature). We chose species that are unicellular (i.e., none were colonial, though some formed cell aggregates), and as morphologically diverse as was possible so as to maximize functional complementarity and facilitate enumeration (similar to (31)).

Experimental Design Given 8 species, it is possible to form $2^8 = 256$ species combinations of any size, and in particular 107 combinations of size 1, 2, 4, and 8. We explored the majority of possible combinations opting to maximize coverage of diversity rather than replication of individual combinations (see Table S1).

Specifically, we assembled 169 communities of 0, 1, 2, 4, or 8 species in transparent sterilized plastic culture flasks (15 mL, optically clear virgin polystyrene); each was labeled and filled with 1,000 cells (except the controls) and algal growth medium to total 15 mL (Alga-Gro® Freshwater Medium, from Carolina Biological Supply Company, Burlington, NC, USA; the algal cultures themselves were also all obtained from Carolina Biological Supply Company). Microcosms were prepared in three batches of equal size, the first one prepared one week before the two others but in otherwise similar conditions, in order to facilitate sampling. The inoculation species densities of 1,000, 500, 250, 125, for 1-, 2-, 4-, 8-species communities, respectively, were prepared from monocultures of known densities. Finally, the microcosms were established under white, full-spectrum lamps for 13 days (corresponding to about 13 generations) at ambient temperature (22°C); this corresponds approximately to their optimal temperature. The microcosms' position under the lamps was randomized daily to minimize effects of possible heterogeneity in the light environment. A conceptual diagram of the experiment is presented in Fig. 1.

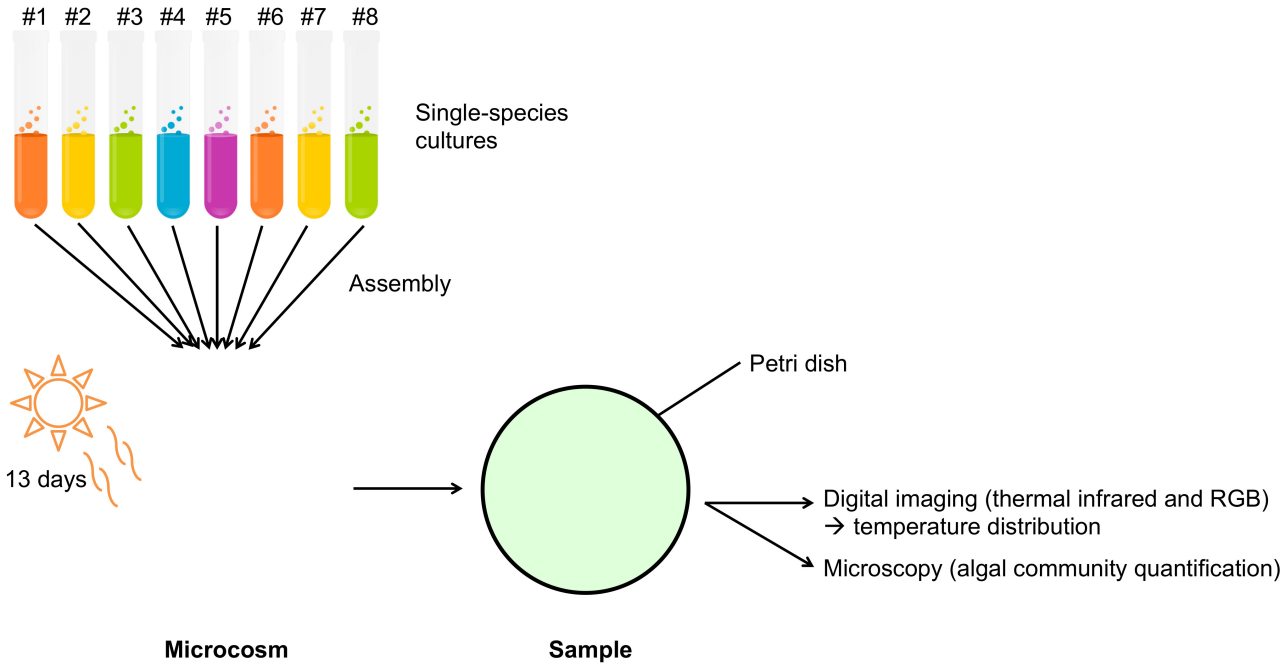

Figure 1. Experimental design: conceptual diagram
RGB refers to red, green, and blue sensors in visible spectrum camera.

Measurement After 13 days of incubation in a nutrient-rich environment and under constant exposure to light, the flasks were vortexed and 1 mL was used for counting (10 photographs of each slide were taken with an inverted microscope at magnification 40x for future counting) and the remaining 14 mL were used to perform thermal imagery. For thermography, the 14 mL samples were individually poured into a Petri dish, promptly covered, and exposed to fiber-optic, low temperature white light (Lumina, Chiu Technical Corporation, Kings Park, NY, USA, 150 W) for 60 seconds (other durations were tested and yielded similar results) to allow algae to absorb light. We removed the lid and took an infrared image with a FLIR T650SC (FLIR Systems, Nashua, NH, USA), as well as a

photograph in the visible spectrum, thus measuring both temperature and visible light (RGB) reflectance of the culture (the color and opacity possibly depending on the density, health and composition of the communities). For the second and third batches (processed together), we also took a thermal image before we heated the culture (which required removing the lid for approximately 5 seconds), inserting our controls at regular intervals between the samples to control for possible warming over the time it took to make measurements. This enabled us to compute ΔT, the temperature change before/after exposure to light ($N = 109$). The control flasks serve as a baseline for the visible and thermal imagery measurements.

Data processing The images obtained by optical microscopy were counted manually. Because of similar morphologies in spite of our efforts to pick dissimilar species (compare Figures S2-S3), we were unable, in many instances, to discriminate among four species when they were in polyculture; these were *Chlamydomonas*, *Chlorella*, *Eudorina* and *Haematococcus*. Where necessary (e.g. in the calculation of complementarity and selection effects), we therefore decided to aggregate the counts of these four species (hereafter referred to as the "isomorphic group" or IG), i.e. in all measures of biovolume and cell count; because of their similar shape, size, chloroplast density, they may share some important functional and ecological features, and obviously have a similar cell volume for purposes of biovolume estimation. From now on, "group" refers to either of the four other species or the isomorphic group (hence five groups). While removing the isomorphic group from the analysis is technically feasible, it accounts for half of the species present. Therefore many species assemblages comprise at least one of those species (87% of our samples), and removing them would reduce the number of (non-control) samples on which to perform the analyses to 20 (down from 164 initially), most of which monocultures. We therefore do not exclude them from our analyses. Nonetheless, and anticipating on the Results section, we note here that we reanalyzed the data where separating the isomorphic group was feasible, e.g. that presented in Tables 1–2, Figures 2–3, since we are using information on the initial composition or on biovolume. The complementarity and selection effects, however, are impossible to compute without lumping together the four species). This did not alter the results. For consistency, we prefer presenting the results for the four species plus isomorphic group throughout the paper.

We estimated biovolume for each group based on the optical microscope images (available in the Supporting Information, Table S2), as data available from different sources on our species' unitary biovolume (the volume of a single cell) seemed not to converge.

Selection and complementarity effects were measured following (16). The selection effect refers to the fact that, given a set of species, a random draw from that pool may select a species with a level of function above average; and thus by increasing diversity (i.e. here, the number of species), one increases the likelihood of picking those high-function species. The complementarity effect, on the other hand, refers to the fact that species may occupy different ecological niches, thus improving resource use efficiency, and may in addition interact in a synergistic (or an antagonistic) way. Overall, these interactions yield a level of function different from what might have been expected by extrapolating function from the monocultures'.

The temperature and RGB (visible spectrum) profiles were extracted from each infrared image using FLIR ExaminIR and ImageJ (Rasband 1997 - 2014) software, and operations on data were conducted in Python with the Python Data Analysis Library (pandas, https://pandas.pydata.org/); the regressions and other statistical tests were run in Stata.

Data analysis The effect of community composition and richness on the RGB profile was assessed, using the mean RGB value of each culture or its standardized value (minus sample average, divided by standard deviation). We examined the effect of several covariates on the maximum and minimum points of the temperature profiles, the (average) temperature after exposition to light, and the amplitude of the change before/after the light treatment – the linear regressions (ordinary least squares, OLS) are described below, and their results are detailed in the next section.

The aforementioned covariates include time trends and a measure of the selection and complementarity effects as defined in (16). The time trends were meant to control for a possible warming over time of the flasks in the measurement room. To learn about the relationship between biovolume and RGB, we estimated the specification

given in Equation (1):

$$\mathrm{RGB}_k = \alpha_0 + \alpha_1(\text{Biovolume})_k + \sum_{f=1}^{F} \alpha_f(\text{Functional Group})_{kf} + \varepsilon_k \quad (1)$$

where $(\text{Biovolume})_k$ is the biovolume measured in flask k, $(\text{Functional Group})_{kf}$ is a dummy for the (initial) presence/absence of the functional group f in flask k; α_0 is the intercept, and ε_k is the error term. The results are presented in Table 2 of the Results section.

To investigate the effect of each hypothesized causal mechanism of influence of biodiversity on temperature (namely: albedo, activity, other unknown channels), we regressed each of our temperature variables on each of the suspected causes, as specified in Equation 2 in its most generic form and fullest specification:

$$\begin{aligned}(\text{Temp})_k = \alpha_0 + \sum_{f=1}^{F} \alpha_f(\text{Functional Group})_{kf} + \lambda_1 \text{Time}_k \times (\text{1st Batch})_k + \lambda_2 \text{Time}_k \times (\text{2nd Batch})_k \\ + \gamma_1 \mathrm{RGB}_k + \gamma_2 (\mathrm{RGB}_k)^2 + \beta_1(\text{Complementarity Effect})_k + \beta_2(\text{Selection Effect})_k + \varepsilon_k \quad (2)\end{aligned}$$

where $Temp$ stands for: ΔT, T_a (the temperature after), T_{min} or T_{max}.

In Equation 2, $(\mathrm{RGB})_k$ is the mean RGB value for flask k, $(\text{Temp})_k$ stands for either T_a (the average temperature of the content of flask k measured *after* exposure to the light source) or ΔT (the temperature *change* before/after exposure) or T_{min} or T_{max} (extreme values measured in the microcosm). $(\text{Functional Group})_{kf}$ is a dummy variable that receives a value of 1 if functional group f is present in flask k for all functional groups. Time_k is a linear time trend for the time at which the flask was analyzed (to account for heating of the room). $(\text{First Batch})_k$ and $(\text{Second Batch})_k$ are dummy variables that receive a value of 1 if the flask belongs to the first or second batch analyzed, respectively. Finally, ε_k is the error term, and α_0 is the regression constant.

The results are discussed in the Results section.

Results

Biodiversity significantly affects productivity

In this study, productivity is measured as the biovolume of the community after 13 days of growth with abundant light and nutrients. As shown on Table 1 and on Fig. S5 (see Supporting Information), the biovolume increases with the richness of the microcosm, but no single species has a significant effect on total biovolume (Table 1).

It should be noted (see Fig. 2) that individual species behaviors are idiosyncratic: for instance, in *Ankistrodesmus* and *Selenastrum* biovolume increases as the number of species increases, but *Cosmarium* did much better in monoculture than in co-culture (in *Ankistrodesmus*, from a median biovolume of about $10^5 \mu m^3$ in monoculture to about $3.10^5 \mu m^3$ in the company of the seven other species, as opposed to *Cosmarium* starting in monoculture with a median biovolume of $3.10^5 \mu m^3$ and a fat upper tail, lower values at $n = 2$ and $n = 4$ and back to about $3.10^5 \mu m^3$ with all 8 species). Interestingly, *Cosmarium* is the species with the highest unitary biovolume.

Our results are overall consistent with the widely observed positive saturating relationship between plant species richness and primary production (3, 29).

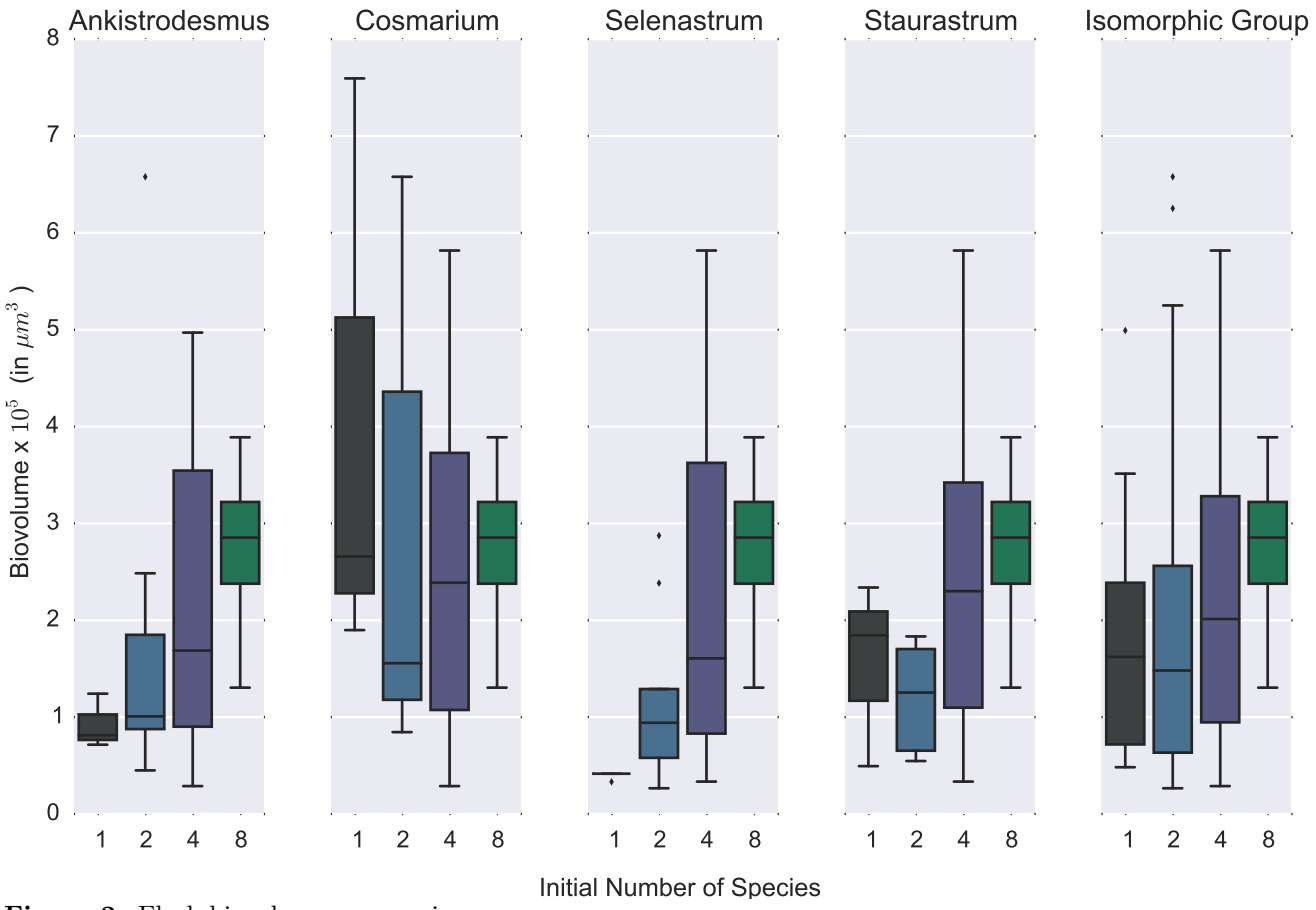

Figure 2. Flask biovolume per species

Each column presents the biovolumes of the flasks containing a particular species, be it as a monoculture or in an assemblage of 2, 4, 8 species. The horizontal line corresponds to the median, the box shows the quartiles, the whiskers describe the rest of the distribution, and the points beyond the whiskers are outliers.

Biovolume significantly affects light absorption

Although it is likely that higher biovolumes would lead to greater visible-spectrum absorbance, there is no reason *a priori* to assume that species-specific volumes and pigment content are correlated. We tested this by estimating the regression described by Equation (1), where mean RGB is regressed against biovolume; the results are summarized in Table 2. Further illustration of this relationship is provided by Fig. S6 of the Supporting Information. The negative relationship between biovolume and RGB is tenuous yet visible on Fig. S6a, reflecting the negative coefficient obtained in column (1) of Table 2. Fig. S6b shows that this relationship persists even when the effect of individual species' presence is controlled for; according to column (2) of Table 2, accounting species identity even strengthens and makes this negative effect become statistically significant at the 10 % level. We note that while 0.1 is not frequently used as a significance level in Ecology, (34) notes that "there is nothing sacred about the value of .05" and that biological significance, rather than statistical significance (while necessary) should be emphasized.

Table 2 also points to the importance of some individual species: the presence of *Selenastrum* seems to increase reflectance – which is consistent with the fact that *Selenastrum* tended to thrive in any combination of species, and therefore produced a lot of biovolume and opacity (apparently not at the expense of the other species) – and the presence of *Cosmarium* seems to decrease light absorption – which is consistent with our observation that *Cosmarium* did, at best, reproduce less than the other genera (and that competition with other genera was in general detrimental to it), thus making the microcosm not as opaque as it could have been.

Adding the initial richness of the microcosm to the initial specification explained more of the variance (Table S3, Fig. 3) than when solely considering the effect of biovolume; the importance of individual species is still supported (see Table S3, though *Cosmarium*'s influence is not significant anymore), but the negative effect of biodiversity (through higher productivity) on the RGB mean is no more. A positive slope is found with the linear specification (column (1) in Table S3 and green line on Fig. 3), and a quadratic specification provides a better fit (column (2) in Table S3 and blue line on Fig. 3), i.e. RGB mean is high in monocultures, decreases in low-diversity mixes, and increases in high-diversity mixes.

Based on these results, the first channel (albedo) of influence of diversity on thermal properties seems valid (though somewhat complex), and appears to be mediated by the system's increased productivity (higher biovolume).

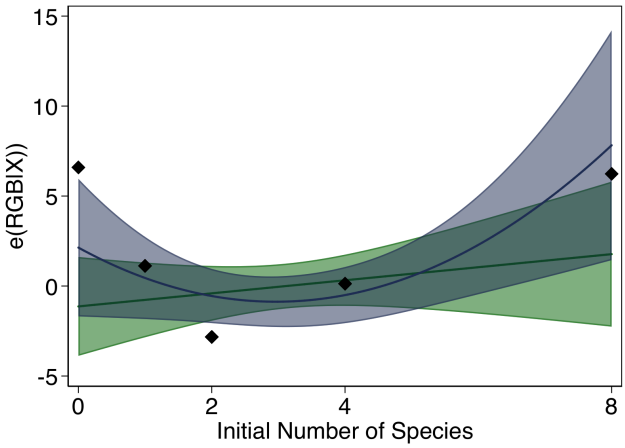

Figure 3. Influence of species richness on visible light reflectance.
Dots represents the mean residual of RGB regressed on the dummies for the functional groups. Solid lines represent a linear fit and quadratic fit, in green and blue, respectively. Shaded areas represent 95% confidence intervals.

Local temperature is not directly influenced by biodiversity

We now turn to the effect of each hypothesized causal mechanism of influence of biodiversity on temperature, and estimated the model described in Equation 2. The temperature variables we considered were T_a (the average temperature of the content of flask k measured *after* exposure to the light source), ΔT (the temperature *change* before/after exposure), T_{min}, and T_{max} (extreme values measured in the microcosm).

We focus here on the results for ΔT, reported in Table 3. The regression tables for the other temperature variables and specifications are consigned in Supporting Information, in tables S4, S5, S6, S7 (T_a, ΔT, T_{max}, T_{min}, respectively, no RGB), S8, S9, S10, S11 (idem, but linear in RGB), S12, S13, S14 (T_a, T_{max}, T_{min}, respectively, quadratic in RGB (full specification)). The distribution of the dependent variables T_a, T_{max}, T_{min} is also available in Supporting Information, Fig. S4. Briefly, Tables S4, S8, S12 show that under the specification used, only the time trends and the presence of *Selenastrum* have a robust and significant effect on the temperature of the microcosms after exposition to light (T_a, $N = 169$). As regards the extreme values of the temperature distribution within the microcosm (T_{min} and T_{max}, $N = 169$), while potentially of ecological significance, they do not seem to be affected in a robust manner by anything other than the time trend. These results are presented in Tables S6-S7, S10-S11, S13-S14. While mean RGB and some genera (those with the largest contribution to biovolume) appear to have a significant effect under some specifications, these effects all disappear when the time trend is taken into account (compare columns (3) and (6) of Tables S10, S11, S13, S14), or when the selection and complementarity effects are included, which makes the reality of these effects doubtful.

If we restrict our analysis to the data of the second batch ($N = 109$), we can compute the temperature difference ΔT (before/after exposition to the source of light), which is more relevant a variable, and proceed to similar regressions (specification following Equation 2 with ΔT as the dependent variable), whose results are reported in Table 3.

Temperature difference is not, unlike the other temperature variables, affected by the warming of the room (the time trend). Rather, as can be seen in Table 3, the reflectance of the suspension, as well as the presence of the isomorphic functional group (IG), are the main drivers of the change in temperature due to exposition to light. The effect of the functional group disappears when selection and complementarity effects are included, but this may be caused by the loss of 20 samples (the monocultures and the controls, for which these variables cannot be computed), thus decreasing statistical power and possibly blurring the picture as a result (lower R^2). We note that the exclusion of 20 samples is likely to have reduced statistical power, so we are cautious in our interpretation of the results. The presence of elements of the IG functional group in the microcosm decreases the temperature change, and this effect seems robust to addition/deletion of controls, see also Table S5). The RGB mean ('albedo') is also an important driver of the magnitude of the temperature change. However, none of the biodiversity effects is significant, in any regression specification we tried.

This absence of a distinct, one-sided, biodiversity effect is also visible in Fig. 4: no clear pattern pertaining to the number of species emerges but for the fact that monoculture extremes (encountered for instance with *Ankistrodesmus*, *Selenastrum* and *Staurastrum*) are tempered by the addition of other species. This seems not to be a dilution effect, judging by the differences between $n = 1$ and $n = 2$ for those species. Therefore, if anything, biodiversity, in our microcosm experiment, dampens the thermal properties of the community.

Fig. 5 summarizes our findings. An increase in species richness increases biovolume (with a constant number of cells at time t=0); an increase in biovolume decreases the mean RGB value; and a decrease in RGB is associated with a decrease in temperature (or possibly an increase in temperature change). However, no empirical evidence supports any effect of biovolume on temperature (change), nor of biodiversity on temperature (change) directly.

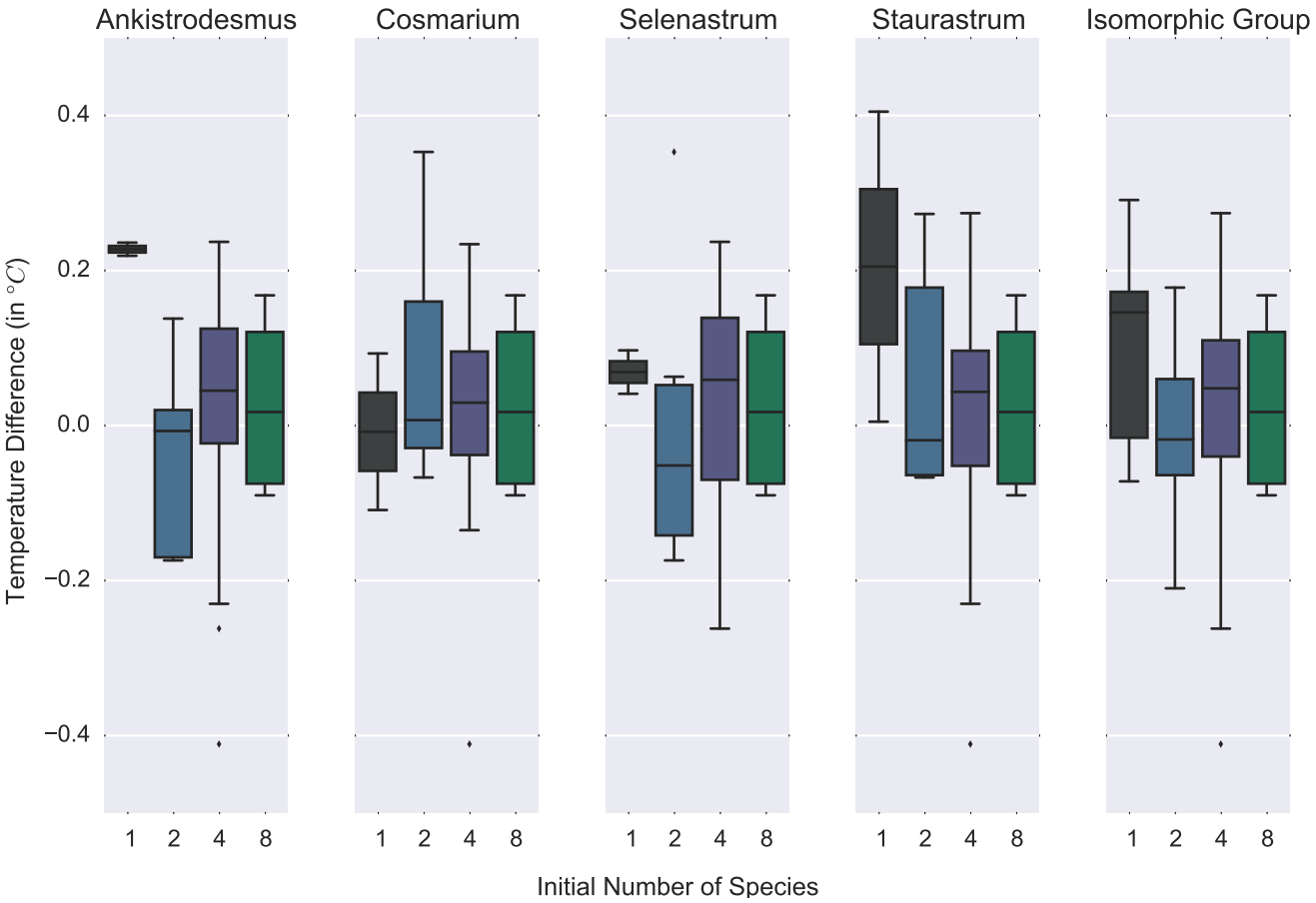

Figure 4. Flask change in temperature, per species

Each column presents the change in temperature (before/after exposition to light) of the flasks containing a particular species, be it as a monoculture or in an assemblage of 2, 4, 8 species. The horizontal line corresponds to the median, the box shows the quartiles, the whiskers describe the rest of the distribution, and the points beyond the whiskers are outliers.

Discussion

Algal species richness in this microcosm study exhibited the positive relationship with primary production observed in many BEF experiments, but showed no direct relationship with the local thermal environmental properties, assessed in this case as the change in temperature, measured by thermography, that occurred after a 60-second exposure to light. Primary production, or algal community biovolume, also did not show a positive relationship with local thermal environmental properties. Instead, the likely causal chain of the influence of diversity over the local thermal environment is through its impact on biovolume and RGB reflectance (color). Fig. 5 summarizes these relationships.

Our study focuses on these issues and illustrates both the approach and complications one may encounter in attempting to identify biodiversity effects that may be subtle or otherwise difficult to detect. We were able to generate a diversity effect on production, as many BEF experiments have found in the past; this change in production had an effect on visible-spectrum absorbance (or, its inverse, reflection, which we measured through RGB imagery). The diversity-induced change in absorbance did impact local temperature, but the effects were weak (low R^2s) and ultimately did not provide a statistically significant link between biodiversity, and the local thermal environment (Fig. 5). The fact that we were unable to find any effect of biodiversity and biovolume on temperature (despite the other relationships found) could indicate that there is indeed no effect, or that our sample size was too small and our experimental protocols too imprecise (in particular, the fact that we were unable to discriminate between genera of the 'IG' functional group). In addition, it should be kept in mind that,

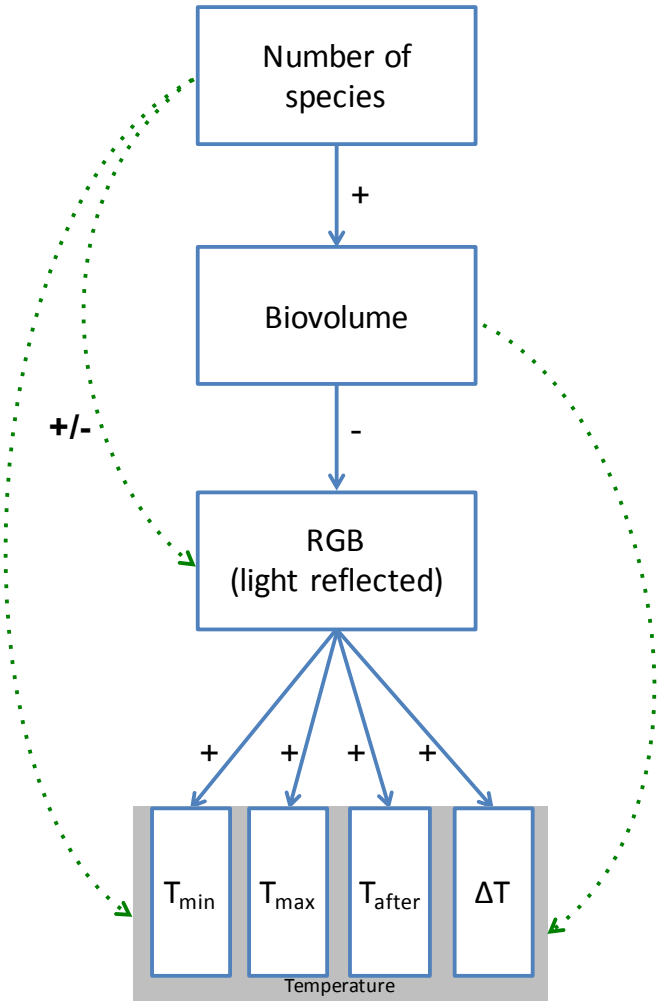

Figure 5. Summary schematic of collective findings and conclusions.
Solid lines represent the statistically significant and unambiguous results, with a plus of minus sign representing the type of the relationship. Dotted lines represent the non-significant relationships. In our microcosms, increased species richness led to an increased biovolume, which in turn led to higher mean RGB (reflectance) values, and higher mean RGB values were significantly associated with higher thermal outcomes: higher ΔT (the temperature difference before/after exposition to light), higher T_a (the temperature difference after exposition to light), higher T_{min} and T_{max} (local extrema).

as any typical BEF experiment, this protocol does not enable to distinguish between "noise" variation (measurement error, etc.) and variation caused by community composition, the latter of which is at play in communities made up of 1 to 4 species, but not 8 (all species).

Given the challenges of measuring potentially subtle effects in algal communities, if one considers that small changes in temperature affect numerous microbial processes in phytoplankton and their associated microbial communities, our findings potentially touch upon important possibilities for the impacts of changing biodiversity on ecosystem functions and properties. It has also been recently noted that microcosm experiments manipulating biodiversity tended to underestimate outcomes occurring in the wild (in terms of community production and stability) (6). Given the vast surface area of freshwater and marine systems and the clarity of the mechanism we identified, even though the direct linkage between diversity and temperature was difficult to detect, the implications are clear. Our results should encourage an alteration in the way albedo is modeled, and go beyond the uniform and time-invariant value attributed to bodies of water, and more generally, to biomes. Such diversity effects could translate to important temperature-mediated biogeochemical consequences at large scales in our world where changes in climate and biodiversity are co-occurring.

Acknowledgments

The authors thank the Thermal Ecology seminar at Columbia University for the fertile scientific atmosphere and their constructive comments, in particular co-instructors Professors Kevin Griffin and Duncan Menge.

Author contributions

All authors contributed equally to this work.

Competing interests

The authors declare no competing interests.

Data Accessibility

Experimental data necessary to reproduce the analyses are made available on Dryad doi:10.5061/dryad.59p3vv5.

References

(1) C. Bellard, C. Bertelsmeier, P. Leadley, W. Thuiller, and F. Courchamp. Impacts of climate change on the future of biodiversity. *Ecology Letters*, 15(4):365–377, 2012. ISSN 1461023X. doi: 10.1111/j.1461-0248.2011.01736.x.

(2) J. Berry and O. Björkman. Photosynthetic response and adaptation to temperature in higher plants. *Annual Review of Plant Physiology*, 98(673):491–543, 1980.

(3) B. J. Cardinale, J. E. Duffy, A. Gonzalez, D. U. Hooper, C. Perrings, P. Venail, A. Narwani, G. M. Mace, D. Tilman, D. A. Wardle, A. P. Kinzig, G. C. Daily, M. Loreau, J. B. Grace, A. Larigauderie, D. S. Srivastava, and S. Naeem. Biodiversity loss and its impact on humanity. *Nature*, 486(7401):59–67, jun 2012. ISSN 1476-4687. doi: 10.1038/nature11148.

(4) R. J. Davies-Colley, R. D. Pridmore, and J. E. Hewitt. Optical properties of some freshwater phytoplanktonic algae. *Hydrobiologia*, 133(2):165–178, 1986. ISSN 00188158. doi: 10.1007/BF00031865.

(5) S. C. Doney, M. Ruckelshaus, J. E. Duffy, J. P. Barry, F. Chan, C. A. English, H. M. Galindo, J. M. Grebmeier, A. B. Hollowed, N. Knowlton, J. Polovina, N. N. Rabalais, W. J. Sydeman, and L. D. Talley. Climate Change Impacts on Marine Ecosystems. *Annual Review of Marine Science*, 4(1):11–37, 2012. ISSN 1941-1405. doi: 10.1146/annurev-marine-041911-111611.

(6) J. E. Duffy, C. M. Godwin, and B. J. Cardinale. Biodiversity effects in the wild are common and as strong as key drivers of productivity. *Nature*, 549(7671):261–264, 2017. ISSN 0028-0836. doi: 10.1038/nature23886.

(7) C. B. Field, D. B. Lobell, H. A. Peters, and N. R. Chiariello. Feedbacks of Terrestrial Ecosystems to Climate Change. *Annual Review of Environment and Resources*, 32(1):1–29, nov 2007. ISSN 1543-5938. doi: 10.1146/annurev.energy.32.053006.141119.

(8) J. A. Foley, J. E. Kutzbach, M. T. Coe, and S. Levis. Feedbacks between climate and boreal forests during the Holocene epoch. *Nature*, 371(6492):52–54, 1994. ISSN 0028-0836. doi: 10.1038/371052a0.

(9) F. C. García, E. Bestion, R. Warfield, and G. Yvon-Durocher. Changes in temperature alter the relationship between biodiversity and ecosystem functioning. *Proceedings of the National Academy of Sciences of the United States of America*, 115(43):10989–10994, 2018. doi: 10.1073/pnas.1805518115.

(10) A. Hector, K. Dobson, A. Minns, E. Bazeley-White, and J. Hartley Lawton. Community diversity and invasion resistance: An experimental test in a grassland ecosystem and a review of comparable studies. *Ecological Research*, 16(5):819–831, 2001. ISSN 0912-3814. doi: 10.1046/j.1440-1703.2001.00443.x.

(11) N. Hoepffner and S. Sathyendranath. Effect of pigment composition on absorption properties of phytoplankton. *Marine Ecology Progress Series*, 73:11–23, 1991. ISSN 0171-8630. doi: 10.3354/meps073011.

(12) IPCC. *Climate Change 2014: Synthesis Report. Contribution of Working Groups I, II and III to the Fifth Assessment Report of the Intergovernmental Panel on Climate Change*. IPCC, Geneva, Switzerland, 2014. ISBN 9789291691432.

(13) X. Irigoien, J. Huisman, and R. P. Harris. Global biodiversity patterns of marine phytoplankton and zooplankton. *Nature*, 429(6994):863–867, 2004. doi: 10.1038/nature02644.1.

(14) J. A. Lathlean and L. Seuront. Infrared thermography in marine ecology: Methods, previous applications and future challenges. *Marine Ecology Progress Series*, 514:263–277, 2014. ISSN 01718630. doi: 10.3354/meps10995.

(15) J. A. Logan, J. Régnière, and J. A. Powell. Assessing the impacts of global warming on forest pest dynamics. *Frontiers in Ecology and the Environment*, 1(3):130–137, 2003. ISSN 15409309. doi: 10.1890/1540-9295(2003)001[0130:ATIOGW]2.0.CO;2.

(16) M. Loreau and A. Hector. Partitioning selection and complementarity in biodiversity experiments. *Nature*, 412:72–76, 2001.

(17) M. Loreau, A. L. Downing, M. C. Emmerson, A. Gonzalez, J. Hughes, P. Inchausti, J. Joshi, J. Norberg, and O. E. Sala. A new look at the relationship between diversity and stability. In M. Loreau, S. Naeem, and P. Inchausti, editors, *Biodiversity and Ecosystem Functioning. Synthesis and Perspectives*, chapter 7, pages 79–91. Oxford University Press, 2002. ISBN 0 19 851570 7 (Hbk).

(18) J. R. Malcolm, C. Liu, R. P. Neilson, L. Hansen, and L. Hannah. Global warming and extinctions of endemic species from biodiversity hotspots. *Conservation Biology*, 20(2):538–548, 2006. ISSN 08888892. doi: 10.1111/j.1523-1739.2006.00364.x.

(19) S. Naeem, L. J. Thompson, S. P. Lawler, J. H. Lawton, and R. M. Woodfin. Declining biodiversity can alter the performance of ecosystems. *Nature*, 368(6473):734–737, 1994. ISSN 0028-0836. doi: 10.1038/368734a0.

(20) S. Naeem, J. E. Duffy, and E. S. Zavaleta. The functions of biological diversity in an age of extinction. *Science*, 336(6087):1401–1406, jun 2012. ISSN 1095-9203. doi: 10.1126/science.1215855.

(21) O. L. Petchey, P. T. McPhearson, T. M. Casey, and P. J. Morin. Environmental warming alters food-web structure and ecosystem function. *Nature*, 402(November):69–72, 1999. ISSN 00280836. doi: 10.1038/47023.

(22) A. Pusceddu, C. Gambi, E. Manini, and R. Danovaro. Trophic state, ecosystem efficiency and biodiversity of transitional aquatic ecosystems: analysis of environmental quality based on different benthic indicators. *Chemistry and Ecology*, 23(6):505–515, 2007. ISSN 0275-7540. doi: 10.1080/02757540701760494.

(23) W. S. Rasband. ImageJ, 1997. URL `http://imagej.nih.gov/ij/docs/index.html`.

(24) A. Ricciardi and J. B. Rasmussen. Extinction Rates of North American Freshwater Fauna. *Conservation Biology*, 13(5):1220–1222, 1999.

(25) L. Seuront, T. P. T. Ng, and J. A. Lathlean. A review of the thermal biology and ecology of molluscs, and of the use of infrared thermography in molluscan research. *Journal of Molluscan Studies*, 84(3):203–232, 2018. ISSN 14643766. doi: 10.1093/mollus/eyy023.

(26) M. P. Thakur, D. Tilman, O. Purschke, M. Ciobanu, J. M. Cowles, F. Isbell, P. D. Wragg, and N. Eisenhauer. Climate warming promotes species diversity, but with greater taxonomic redundancy, in complex environments. *Science Advances*, 3(e1700866):1–10, 2017.

(27) D. Tilman, D. Wedin, and J. M. H. Knops. Productivity and sustainability influenced by biodiversity in grassland ecosystems. *Nature*, 379(6567):718–720, 1996.

(28) D. Tilman, P. B. Reich, and J. M. H. Knops. Biodiversity and ecosystem stability in a decade-long grassland experiment. *Nature*, 441(7093):629–32, jun 2006. ISSN 1476-4687. doi: 10.1038/nature04742.

(29) D. Tilman, F. Isbell, and J. M. Cowles. Biodiversity and Ecosystem Functioning. *Annual Review of Ecology, Evolution, and Systematics*, 45:471–93, 2014. ISSN 1543-592X. doi: 10.1126/science.1064088.

(30) S. M. Vallina, M. J. Follows, S. Dutkiewicz, J. M. Montoya, P. Cermeno, and M. Loreau. Global relationship between phytoplankton diversity and productivity in the ocean. *Nature Communications*, 5:4299, 2014. doi: 10.1038/ncomms5299.

(31) J. J. Weis, D. S. Madrigal, and B. J. Cardinale. Effects of algal diversity on the production of biomass in homogeneous and heterogeneous nutrient environments: A microcosm experiment. *PLoS ONE*, 3(7):e2825, 2008. ISSN 19326203. doi: 10.1371/journal.pone.0002825.

(32) T. Wernberg, D. A. Smale, and M. S. Thomsen. A decade of climate change experiments on marine organisms: procedures, patterns and problems. *Global Change Biology*, 18(5):1491–1498, 2012. ISSN 13541013. doi: 10.1111/j.1365-2486.2012.02656.x.

(33) K. J. Willis and G. M. MacDonald. Long-Term Ecological Records and Their Relevance to Climate Change Predictions for a Warmer World. *Annual Review of Ecology, Evolution, and Systematics*, 42(1):267–287, 2011. ISSN 1543-592X. doi: 10.1146/annurev-ecolsys-102209-144704.

(34) N. G. Yoccoz. Use, Overuse, and Misuse of Significance Tests in Evolutionary Biology and Ecology. *Bulletin of the Ecological Society of America*, 72(2):106–111, 1991.

Tables

Table 1. Influence of microcosm composition on biovolume. Each column corresponds to a separate regression: the independent variables are, in column (1), species richness (linear), in column (2), a quadratic in species richness, in column (3), species richness (linear) and dummies (indicator functions) indicating the presence/absence of each group in the initial species mixture, in column (4), a quadratic in species richness and the group dummies.

Notes: $*p < 0.1, **p < 0.05, ***p < 0.01$. $N = 162$. Robust standard errors are indicated in parentheses.

Dependent Variable: Biovolume

	(1)	(2)	(3)	(4)
$N_{Species}$	19704.682***	34765.725*	24697.360*	43228.318*
	(6556.075)	(17619.573)	(12963.029)	(24767.124)
$N^2_{Species}$		-2141.077		-2179.164
		(1982.076)		(2244.786)
Ankistrodesmus			-39205.166	-42324.962
			(26992.927)	(26806.441)
Cosmarium			49323.755	46096.612
			(33073.750)	(33004.238)
Selenastrum			-38465.483	-41133.504
			(27172.388)	(27390.329)
Staurastrum			-21112.737	-23953.073
			(27379.180)	(27880.794)
Isomorphic Group			12150.509	-3248.527
			(44893.394)	(50141.158)
Constant	139032.475***	118424.819***	131024.894***	117830.291***
	(25403.689)	(35827.400)	(36880.235)	(38599.427)
R^2	0.046	0.050	0.107	0.111

Table 2. Regression: species presence and biovolume effect on standardized RGBEach column corresponds to a separate regression on standardized RGB: the independent variables are, in column (1), standardized biovolume, in column (2), standardized biovolume and group dummies (signalling the initial presence/absence of each group in the microcosm).

Notes: $*p < 0.1, **p < 0.05, ***p < 0.01$. Robust standard errors in parentheses.

Dependent Variable: Standardized RGB

	(1)	(2)
Standardized Biovolume	-0.107	-0.140*
	(0.077)	(0.079)
Ankistrodesmus		-0.253
		(0.167)
Cosmarium		0.292*
		(0.160)
Selenastrum		-0.392**
		(0.155)
Staurastrum		0.084
		(0.165)
Isomorphic Group		-0.292
		(0.246)
Constant	0.005	0.353
	(0.079)	(0.250)
R^2	0.011	0.099
N	162	162

Table 3. Regression results: Influence of microcosm composition and greenness on ΔT. Each column corresponds to a separate regression on ΔT: the independent variables are, in column (1), a quadratic in RGB mean, in column (2), a quadratic in RGB mean and group dummies, in column (3), a quadratic in RGB mean, group dummies and a time trend, in column (4), selection and complementarity effects only, in column (5), a quadratic in RGB mean, group dummies, selection and complementarity effects, in column (6), a quadratic in RGB mean, group dummies, a time trend, selection and complementarity effects.

Notes: $*p < 0.1, **p < 0.05, ***p < 0.01$. Robust standard errors in parentheses.

Dependent Variable: Temperature Difference (°C)

	(1)	(2)	(3)	(4)	(5)	(6)
(RGB Mean)	0.068	0.202***	0.200***		0.180**	0.184**
	(0.066)	(0.071)	(0.071)		(0.089)	(0.089)
(RGB Mean)^2	-0.000	-0.001***	-0.001***		-0.001**	-0.001**
	(0.000)	(0.000)	(0.000)		(0.000)	(0.000)
Ankistrodesmus		0.007	0.008		-0.002	-0.001
		(0.025)	(0.025)		(0.031)	(0.031)
Cosmarium		-0.027	-0.024		-0.023	-0.016
		(0.025)	(0.026)		(0.032)	(0.034)
Selenastrum		-0.008	-0.003		0.003	0.011
		(0.028)	(0.031)		(0.031)	(0.035)
Staurastrum		-0.006	-0.001		-0.007	-0.000
		(0.027)	(0.028)		(0.030)	(0.031)
Isomorphic Group		-0.128***	-0.121***		-0.097	-0.083
		(0.043)	(0.045)		(0.073)	(0.072)
Time Trend Second Batch			-0.000			-0.000
			(0.000)			(0.000)
Selection Effect				0.000	-0.000	-0.000
				(0.000)	(0.000)	(0.000)
Complementarity Effect				0.000	-0.000	-0.000
				(0.000)	(0.000)	(0.000)
Constant	-4.868	-14.029***	-13.845***	0.015	-12.566**	-12.849**
	(4.620)	(4.968)	(4.952)	(0.022)	(6.168)	(6.213)
R^2	0.019	0.121	0.123	0.006	0.078	0.081
N	109	109	109	84	84	84

Figure Legends

Figure 1. Experimental design: conceptual diagram RGB refers to red, green, and blue sensors in visible spectrum camera.

Figure 2. Flask biovolume per species Each column presents the biovolumes of the flasks containing a particular species, be it as a monoculture or in an assemblage of 2, 4, 8 species. The horizontal line corresponds to the median, the box shows the quartiles, the whiskers describe the rest of the distribution, and the points beyond the whiskers are outliers.

Figure 3. Influence of species richness on visible light reflectance Dots represents the mean residual of RGB regressed on the dummies for the functional groups. Solid lines represent a linear fit and quadratic fit, in green and blue, respectively. Shaded areas represent 95% confidence intervals.

Figure 4. Flask change in temperature, per species Each column presents the change in temperature (before/after exposition to light) of the flasks containing a particular species, be it as a monoculture or in an assemblage of 2, 4, 8 species. The horizontal line corresponds to the median, the box shows the quartiles, the whiskers describe the rest of the distribution, and the points beyond the whiskers are outliers.

Figure 5. Summary schematic of collective findings and conclusions Solid lines represent the statistically significant and unambiguous results, with a plus of minus sign representing the type of the relationship. Dotted lines represent the non-significant relationships. In our microcosms, increased species richness led to an increased biovolume, which in turn led to higher mean RGB (reflectance) values, and higher mean RGB values were significantly associated with higher thermal outcomes: higher ΔT (the temperature difference before/after exposition to light), higher T_a (the temperature difference after exposition to light), higher T_{min} and T_{max} (local extrema).

Supporting Information

Additional experimental details

Timing of the experiment The first batch of microcosms was assembled on November 26$^{\text{th}}$, 2014, and the last series of microcosms were imaged on December 15$^{\text{th}}$, 2014, allowing for a 13 day incubation period for all the microcosms.

Sampling schedule and processing The first batch of microcosms was prepared on November 26$^{\text{th}}$, 2014, and sacrificed 13 days later (i.e. December 9$^{\text{th}}$): thermal and visible imagery was conducted, and samples were subsequently disposed of. The second and third batches were prepared in the same fashion together on December 2$^{\text{nd}}$, 2014, and imaged together on December 15$^{\text{th}}$, 13 days after assembly as well. Thirteen days was the duration required to ascertain reasonable (observable) growth was taking place; it is consistent with the duration specified on growth medium for "most algae [to] show substantial growth". Before assembly, the pure algal strands were stored at room temperature under a 24 W T5 fluorescent lamp. After assembly, the microcosms were stored at room temperature and were shuffled daily to homogenize exposition to light.

S1 Table

Table S1. Community combinatorics.

	C_n^k	replicates	nb. microcosms
0 species (control)	1		5
1 species	8	8 triplicates	24
2 species	28	12 duplicates, 16 singles	70
4 species	70	24 duplicates, 46 singles	54
8 species	1	1 sextuplicate	6
Total			169

Species information

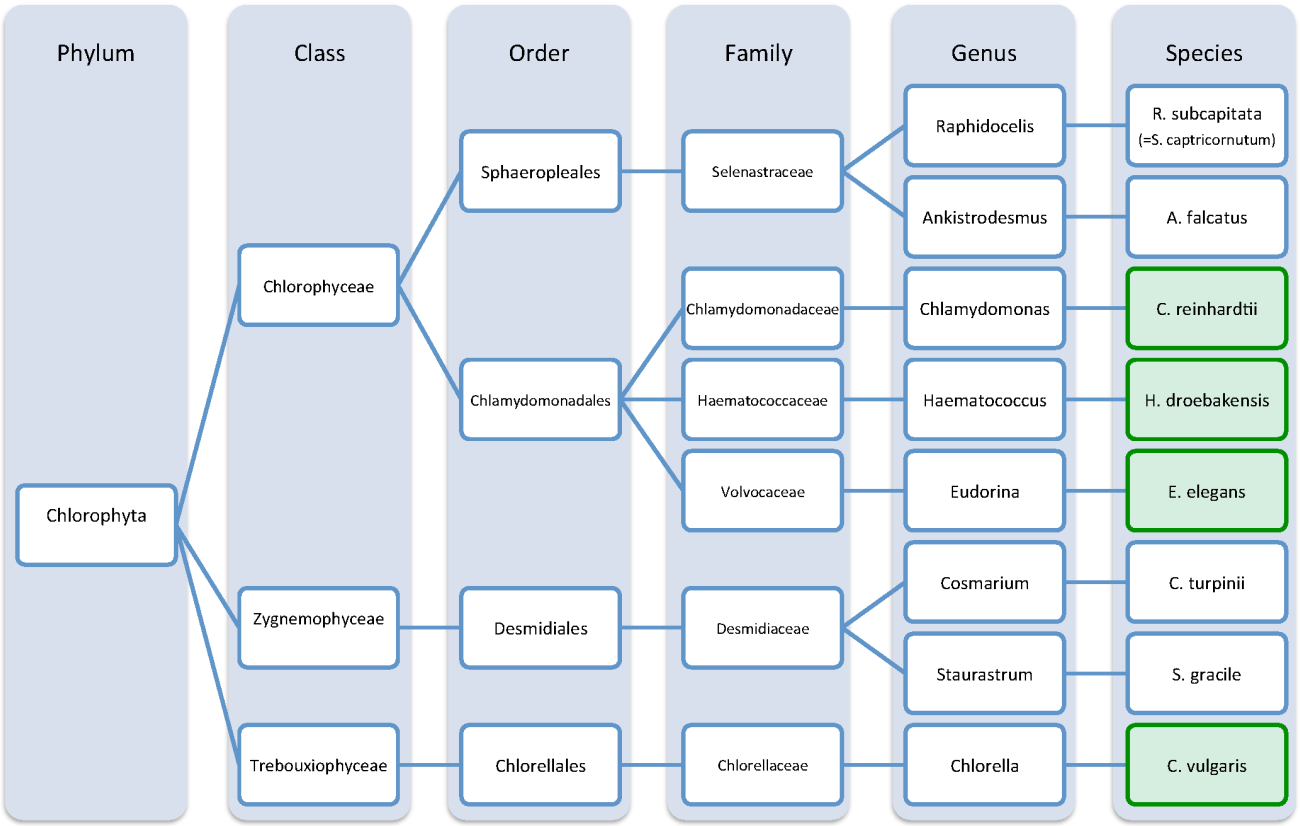

Figure S1. Phylogenetic information.

Phylogenetic relationships of the eight species used. Shadowed in green: the four isomorphic species.

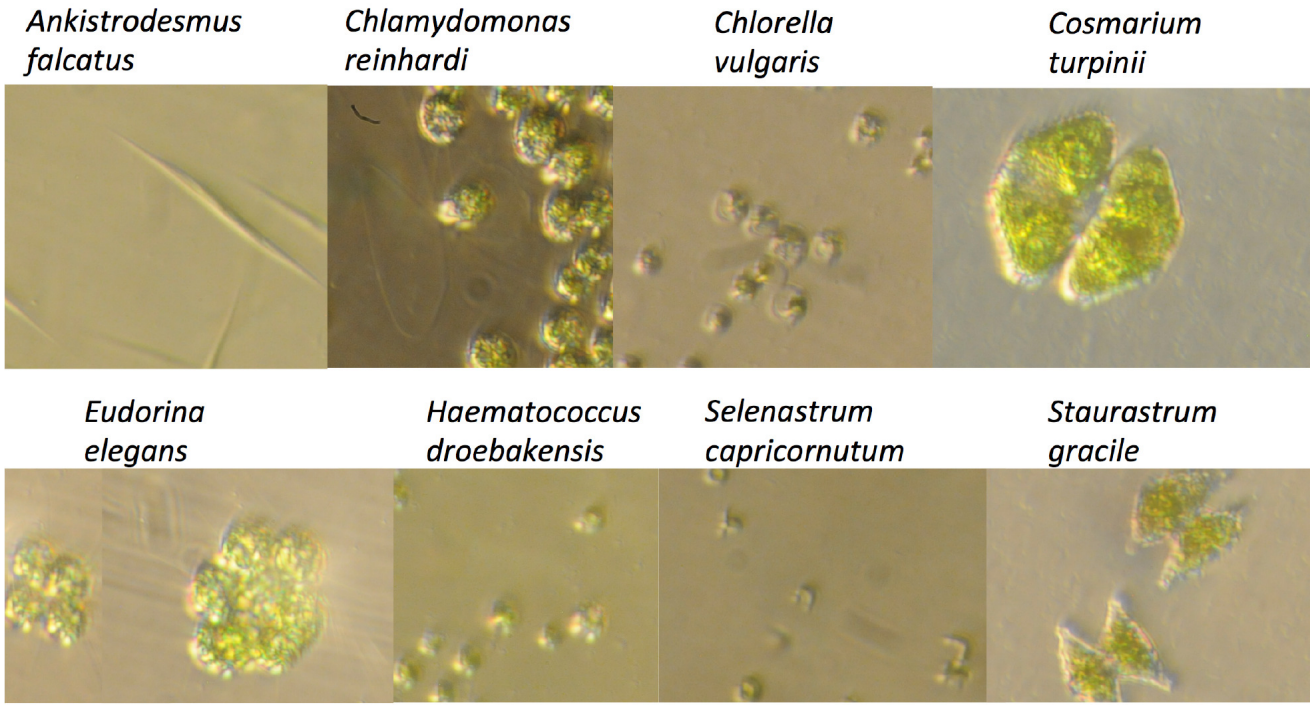

Figure S2. Algal morphology.
Plate used for species identification.

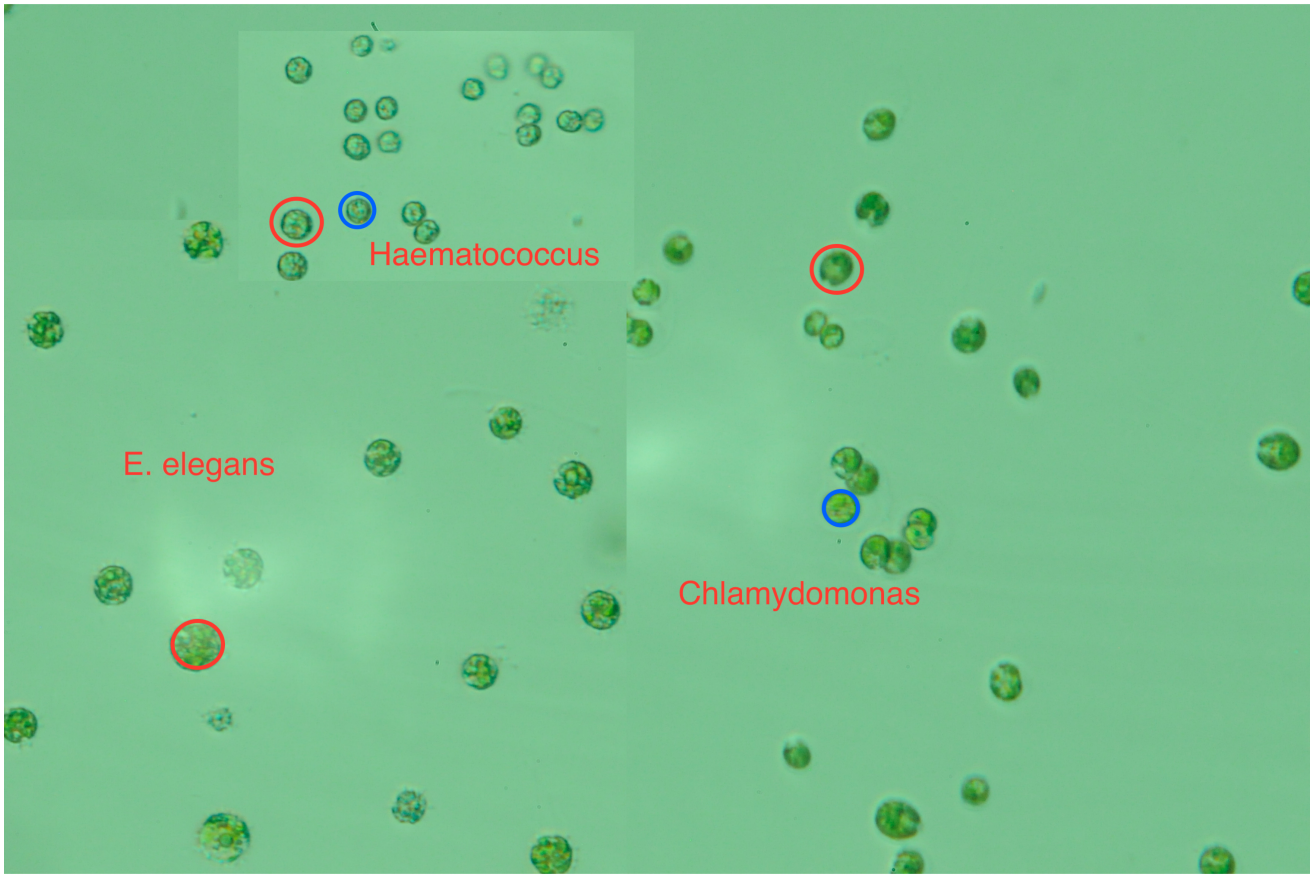

Figure S3. Algal morphology, experimental conditions.
Mosaic of photographs of slides under inverted microscope at magnification 40x, used for enumeration. Annotated to highlight morphological closeness between *Chlamydomonas*, *E. elegans*, *Haematococcus*.

Empirical biovolumes

Table S2. Biovolumes

Species	Biovolume (μm^3)	replicates	Std. err.
Ankistrodesmus falcatus	116	75	9.9
Chlamydomonas reinhardtii	313	75	21.7
Chlorella vulgaris	95	75	8.1
Cosmarium turpinii	33 226	20	2 355.8
Eudorina elegans	456	75	46.2
Haematococcus droebakensis	154	75	10.2
Selenastrum capricornutum	45	75	2.9
Staurastrum gracile	2 882	20	196.5

Temperature distributions in the sample

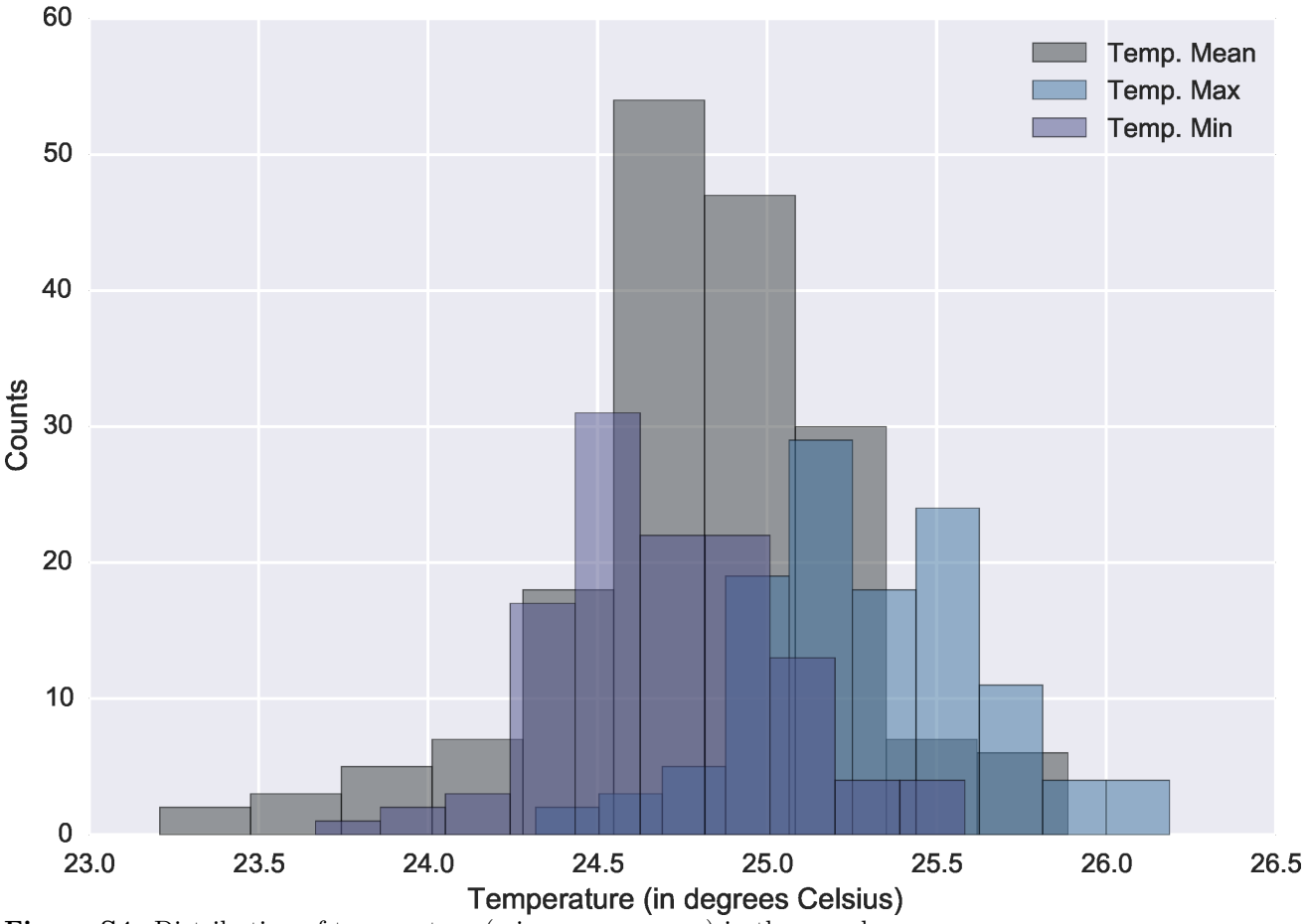

Figure S4. Distribution of temperature (min, max, average) in the sample.

Species richness is positively correlated to biovolume

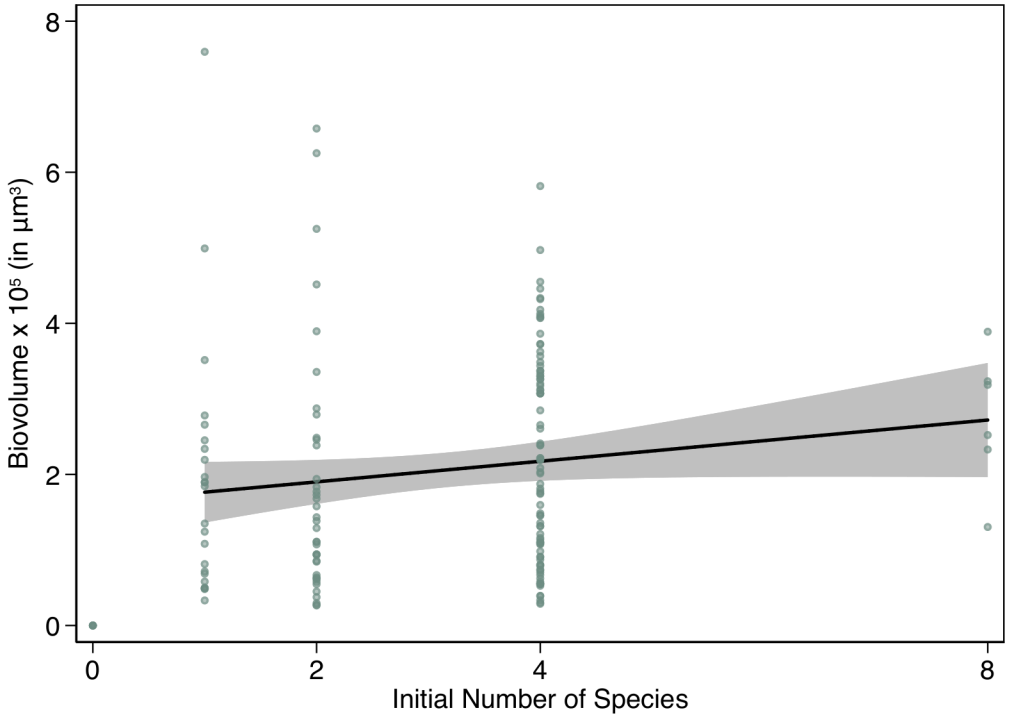

Figure S5. Microcosm biovolume and initial species richness
Solid line represents the linear best fit of the measured biovolume as a function of the number of initial species. Shaded area represents 95% confidence intervals.

Biovolume is negatively correlated to RGB

In both regressions presented in Table 2, biovolume is negatively associated with RGB values (albeit insignificantly so in Column (1)). Column (2) shows that this relationship persists, and is strengthened (i.e. becomes significant at the 10% level), when the effect of individual species' presence is controlled for. Note that Column (2) also points to the importance of some individual species: the presence of *Selenastrum* seems to increase "greenness" – which is consistent with the fact that *Selenastrum* tended to thrive in any combination of species, and therefore produced a lot of biovolume and opacity (apparently not at the expense of the other species) – and the presence of *Cosmarium* seems to decrease light absorption – which is consistent with our observation that *Cosmarium* did, at best, reproduce less than the other genera (and that competition with other genera was in general detrimental to it), thus making the microcosm not as opaque as it could have been.

Fig. S6a shows the RGB values versus the biovolume (analogous to Column (1) of Table 2), and hints at a negative but weak relationship between biovolume and RGB; on Fig. S6b are plotted the residuals from the regression of RGB on the functional group dummies, against the residuals from biovolume on the functional group dummies – i.e. a partial regression plot – which shows that the negative slope persists even when the effect of individual species' presence is subtracted from both biovolume and RGB (mirroring the findings of Column (2) in Table 2).

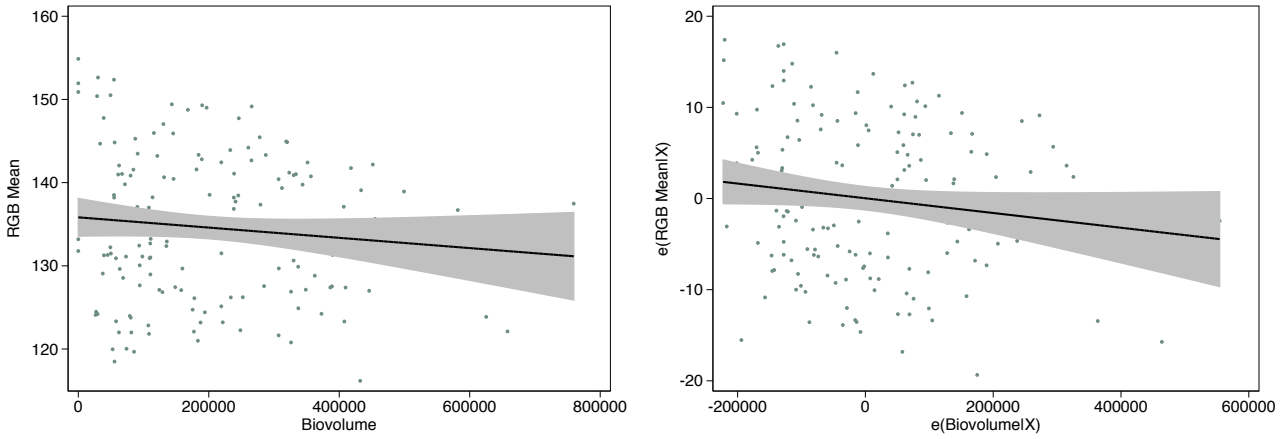

(a) Scatter Plot **(b)** Partial Regression Plot

Figure S6. Influence of biovolume on RGB Mean

Scatter plot and the partial regression plot showing the negative linear relationship between the mean RGB and biovolume. Solid line shows the linear best fit. Shaded area shows the 95% confidence intervals.

There is a quadratic relationship between species richness and RGB

Table S3. Regression results: Microcosm composition and RGB mean value.

Notes: $*p < 0.1, **p < 0.05, ***p < 0.01$

Dependent Variable: RGB Mean

	(1)	(2)
$N_{Species}$	1.487**	-1.315
	(0.750)	(1.431)
$N^2_{Species}$		0.330**
		(0.162)
Ankistrodesmus	-3.682**	-3.170**
	(1.521)	(1.502)
Cosmarium	0.297	0.846
	(1.511)	(1.497)
Selenastrum	-4.827***	-4.402***
	(1.358)	(1.366)
Staurastrum	-1.310	-0.862
	(1.644)	(1.641)
Isomorphic Group	-5.310**	-3.069
	(2.474)	(2.469)
Constant	138.099***	140.139***
	(2.097)	(2.312)
R^2	0.100	0.123
N	169	169

Other regressions

Table S4. Regression results: Microcosm composition and T_a.

Notes: $*p < 0.1, **p < 0.05, ***p < 0.01$. Robust standard errors in parentheses.

Dependent Variable: Temperature After (°C)

	(1)	(2)	(3)	(4)	(5)
Ankistrodesmus	-0.085	-0.104*		-0.082	-0.093
	(0.070)	(0.053)		(0.087)	(0.071)
Cosmarium	-0.004	-0.047		0.023	-0.045
	(0.071)	(0.059)		(0.082)	(0.072)
Selenastrum	0.102	0.120**		0.115	0.137*
	(0.070)	(0.059)		(0.079)	(0.072)
Staurastrum	0.088	0.079		0.115	0.090
	(0.069)	(0.062)		(0.085)	(0.077)
Isomorphic Group	-0.020	-0.001		0.000	-0.009
	(0.060)	(0.070)		(0.114)	(0.120)
Time Trend First Batch		-0.001***			-0.001**
		(0.000)			(0.000)
Time Trend Second Batch		0.000***			0.001***
		(0.000)			(0.000)
Selection Effect			-0.000	-0.000	0.000
			(0.000)	(0.000)	(0.000)
Complementarity Effect			-0.000	-0.000	0.000
			(0.000)	(0.000)	(0.000)
Constant	24.779***	24.726***	24.846***	24.771***	24.629***
	(0.058)	(0.066)	(0.074)	(0.153)	(0.156)
R^2	0.030	0.396	0.009	0.048	0.429
N	169	169	129	129	129

Table S5. Regression results: Microcosm composition and ΔT.

Notes: $*p < 0.1, **p < 0.05, ***p < 0.01$. Robust standard errors in parentheses.

Dependent Variable: Temperature Difference (°C)

	(1)	(2)	(3)	(4)	(5)
Ankistrodesmus	-0.006	-0.005		-0.011	-0.011
	(0.027)	(0.027)		(0.031)	(0.031)
Cosmarium	-0.015	-0.012		-0.002	0.000
	(0.025)	(0.027)		(0.032)	(0.034)
Selenastrum	-0.010	-0.007		0.002	0.003
	(0.027)	(0.028)		(0.029)	(0.032)
Staurastrum	0.002	0.006		0.001	0.003
	(0.027)	(0.030)		(0.029)	(0.032)
Isomorphic Group	-0.081*	-0.076*		-0.052	-0.048
	(0.043)	(0.043)		(0.080)	(0.080)
Time Trend Second Batch		-0.000			-0.000
		(0.000)			(0.000)
Selection Effect			0.000	0.000	0.000
			(0.000)	(0.000)	(0.000)
Complementarity Effect			0.000	0.000	0.000
			(0.000)	(0.000)	(0.000)
Constant	0.116***	0.124**	0.015	0.066	0.068
	(0.043)	(0.049)	(0.022)	(0.091)	(0.094)
R^2	0.057	0.058	0.006	0.019	0.020
N	109	109	84	84	84

Table S6. Regression results: Microcosm composition and T_{max}.

Notes: $*p < 0.1, **p < 0.05, ***p < 0.01$. Robust standard errors in parentheses.

Dependent Variable: Temperature Maximum (°C)

	(1)	(2)	(3)	(4)	(5)
Ankistrodesmus	-0.094	-0.114**		-0.092	-0.105
	(0.072)	(0.053)		(0.089)	(0.072)
Cosmarium	-0.001	-0.053		0.029	-0.055
	(0.073)	(0.059)		(0.084)	(0.071)
Selenastrum	0.093	0.106*		0.100	0.113
	(0.072)	(0.058)		(0.081)	(0.072)
Staurastrum	0.080	0.063		0.105	0.067
	(0.071)	(0.062)		(0.088)	(0.078)
Isomorphic Group	-0.020	-0.007		0.016	-0.018
	(0.062)	(0.067)		(0.123)	(0.131)
Time Trend First Batch		-0.001***			-0.001**
		(0.000)			(0.000)
Time Trend Second Batch		0.001***			0.001***
		(0.000)			(0.000)
Selection Effect			-0.000	-0.000	0.000
			(0.000)	(0.000)	(0.000)
Complementarity Effect			-0.000	-0.000	0.000
			(0.000)	(0.000)	(0.000)
Constant	25.098***	25.033***	25.162***	25.089***	24.931***
	(0.060)	(0.064)	(0.076)	(0.162)	(0.163)
R^2	0.026	0.427	0.010	0.044	0.448
N	169	169	129	129	129

Table S7. Regression results: Microcosm composition and T_{min}.

Notes: $*p < 0.1, **p < 0.05, ***p < 0.01$. Robust standard errors in parentheses.

Dependent Variable: Temperature Minimum (°C)

	(1)	(2)	(3)	(4)	(5)
Ankistrodesmus	-0.069	-0.085		-0.065	-0.075
	(0.066)	(0.052)		(0.082)	(0.069)
Cosmarium	-0.024	-0.059		-0.001	-0.065
	(0.068)	(0.058)		(0.078)	(0.070)
Selenastrum	0.086	0.105*		0.096	0.114
	(0.066)	(0.058)		(0.074)	(0.072)
Staurastrum	0.079	0.075		0.104	0.079
	(0.066)	(0.061)		(0.081)	(0.076)
Isomorphic Group	-0.026	-0.005		-0.013	-0.026
	(0.057)	(0.068)		(0.105)	(0.114)
Time Trend First Batch		-0.001***			-0.001**
		(0.000)			(0.000)
Time Trend Second Batch		0.000***			0.001***
		(0.000)			(0.000)
Selection Effect			-0.000	-0.000	0.000
			(0.000)	(0.000)	(0.000)
Complementarity Effect			-0.000	-0.000	0.000
			(0.000)	(0.000)	(0.000)
Constant	24.546***	24.505***	24.585***	24.535***	24.406***
	(0.055)	(0.064)	(0.071)	(0.141)	(0.146)
R^2	0.025	0.346	0.008	0.040	0.382
N	169	169	129	129	129

Table S8. Regression results: mean RGB and T_a (linear).

Notes: $*p < 0.1, **p < 0.05, ***p < 0.01$. Robust standard errors in parentheses.

Dependent Variable: Temperature After (°C)

	(1)	(2)	(3)	(4)	(5)	(6)
(RGB Mean)	0.020***	0.022***	-0.001		0.027***	-0.001
	(0.004)	(0.004)	(0.005)		(0.005)	(0.006)
Ankistrodesmus		-0.038	-0.108*		-0.066	-0.093
		(0.063)	(0.056)		(0.079)	(0.072)
Cosmarium		-0.049	-0.048		-0.074	-0.044
		(0.065)	(0.059)		(0.073)	(0.072)
Selenastrum		0.176***	0.115*		0.173**	0.135*
		(0.066)	(0.064)		(0.075)	(0.077)
Staurastrum		0.081	0.077		0.083	0.089
		(0.061)	(0.063)		(0.073)	(0.078)
Isomorphic Group		0.039	-0.006		-0.051	-0.009
		(0.073)	(0.070)		(0.173)	(0.119)
Time Trend First Batch			-0.001***			-0.001**
			(0.000)			(0.000)
Time Trend Second Batch			0.000***			0.001**
			(0.000)			(0.000)
Selection Effect				-0.000	-0.000	0.000
				(0.000)	(0.000)	(0.000)
Complementarity Effect				-0.000	-0.000	0.000
				(0.000)	(0.000)	(0.000)
Constant	22.084***	21.689***	24.918***	24.846***	21.166***	24.727***
	(0.489)	(0.550)	(0.635)	(0.074)	(0.659)	(0.787)
R^2	0.157	0.207	0.396	0.009	0.269	0.429
N	169	169	169	129	129	129

Table S9. Regression results: mean RGB and ΔT (linear).

Notes: $*p < 0.1, **p < 0.05, ***p < 0.01$. Robust standard errors in parentheses.

Dependent Variable: Temperature Difference (°C)

	(1)	(2)	(3)	(4)	(5)	(6)
(RGB Mean)	0.002	0.002	0.002		0.003	0.003
	(0.002)	(0.002)	(0.002)		(0.003)	(0.003)
Ankistrodesmus		-0.004	-0.002		-0.012	-0.011
		(0.026)	(0.026)		(0.031)	(0.031)
Cosmarium		-0.019	-0.014		-0.013	-0.007
		(0.026)	(0.027)		(0.033)	(0.034)
Selenastrum		-0.003	0.005		0.010	0.016
		(0.028)	(0.031)		(0.030)	(0.035)
Staurastrum		-0.001	0.006		-0.006	-0.000
		(0.028)	(0.030)		(0.030)	(0.032)
Isomorphic Group		-0.077*	-0.067		-0.058	-0.046
		(0.044)	(0.045)		(0.078)	(0.078)
Time Trend Second Batch			-0.000			-0.000
			(0.000)			(0.000)
Selection Effect				0.000	-0.000	0.000
				(0.000)	(0.000)	(0.000)
Complementarity Effect				0.000	0.000	0.000
				(0.000)	(0.000)	(0.000)
Constant	-0.242	-0.106	-0.170	0.015	-0.343	-0.371
	(0.274)	(0.304)	(0.324)	(0.022)	(0.355)	(0.374)
R^2	0.010	0.062	0.066	0.006	0.036	0.038
N	109	109	109	84	84	84

Table S10. Regression results: mean RGB and T_{max} (linear).

Notes: $*p < 0.1, **p < 0.05, ***p < 0.01$. Robust standard errors in parentheses.

Dependent Variable: Temperature Maximum (°C)

	(1)	(2)	(3)	(4)	(5)	(6)
(RGB Mean)	0.022***	0.024***	-0.001		0.029***	-0.001
	(0.004)	(0.004)	(0.005)		(0.005)	(0.006)
Ankistrodesmus		-0.043	-0.117**		-0.076	-0.105
		(0.063)	(0.055)		(0.080)	(0.072)
Cosmarium		-0.049	-0.053		-0.075	-0.054
		(0.066)	(0.059)		(0.075)	(0.071)
Selenastrum		0.173**	0.102		0.162**	0.111
		(0.067)	(0.064)		(0.076)	(0.077)
Staurastrum		0.073	0.062		0.070	0.066
		(0.063)	(0.063)		(0.075)	(0.079)
Isomorphic Group		0.044	-0.011		-0.039	-0.018
		(0.074)	(0.067)		(0.178)	(0.130)
Time Trend First Batch			-0.001***			-0.001**
			(0.000)			(0.000)
Time Trend Second Batch			0.001***			0.001***
			(0.000)			(0.000)
Selection Effect				-0.000	-0.000	0.000
				(0.000)	(0.000)	(0.000)
Complementarity Effect				-0.000	-0.000	0.000
				(0.000)	(0.000)	(0.000)
Constant	22.123***	21.737***	25.179***	25.162***	21.254***	25.030***
	(0.496)	(0.555)	(0.634)	(0.076)	(0.670)	(0.788)
R^2	0.181	0.227	0.427	0.010	0.281	0.448
N	169	169	169	129	129	129

Table S11. Regression results: mean RGB and T_{min} (linear).

Notes: $*p < 0.1, **p < 0.05, ***p < 0.01$. Robust standard errors in parentheses.

Dependent Variable: Temperature Minimum (°C)

	(1)	(2)	(3)	(4)	(5)	(6)
(RGB Mean)	0.018***	0.020***	-0.001		0.025***	0.000
	(0.004)	(0.004)	(0.005)		(0.005)	(0.006)
Ankistrodesmus		-0.028	-0.087		-0.051	-0.075
		(0.060)	(0.055)		(0.075)	(0.070)
Cosmarium		-0.064	-0.059		-0.090	-0.065
		(0.062)	(0.058)		(0.070)	(0.071)
Selenastrum		0.151**	0.103		0.149**	0.114
		(0.063)	(0.064)		(0.071)	(0.076)
Staurastrum		0.073	0.074		0.075	0.079
		(0.059)	(0.062)		(0.070)	(0.077)
Isomorphic Group		0.026	-0.007		-0.059	-0.026
		(0.071)	(0.069)		(0.160)	(0.115)
Time Trend First Batch			-0.001***			-0.001**
			(0.000)			(0.000)
Time Trend Second Batch			0.000**			0.001**
			(0.000)			(0.000)
Selection Effect				-0.000	-0.000	0.000
				(0.000)	(0.000)	(0.000)
Complementarity Effect				-0.000	0.000	0.000
				(0.000)	(0.000)	(0.000)
Constant	22.139***	21.793***	24.603***	24.585***	21.273***	24.403***
	(0.476)	(0.530)	(0.646)	(0.071)	(0.622)	(0.804)
R^2	0.138	0.183	0.346	0.008	0.244	0.382
N	169	169	169	129	129	129

Table S12. Regression results: mean RGB and T_a (quadratic).

Notes: $*p < 0.1, **p < 0.05, ***p < 0.01$. Robust standard errors in parentheses.

Dependent Variable: Temperature After (°C)

	(1)	(2)	(3)	(4)	(5)	(6)
(RGB Mean)	0.338***	0.325***	0.098		0.398***	0.114
	(0.094)	(0.101)	(0.098)		(0.137)	(0.124)
(RGB Mean)^2	-0.001***	-0.001***	-0.000		-0.001***	-0.000
	(0.000)	(0.000)	(0.000)		(0.001)	(0.000)
Ankistrodesmus		-0.019	-0.098*		-0.047	-0.086
		(0.063)	(0.056)		(0.077)	(0.072)
Cosmarium		-0.042	-0.047		-0.053	-0.039
		(0.063)	(0.059)		(0.073)	(0.071)
Selenastrum		0.148**	0.107*		0.136*	0.126
		(0.065)	(0.065)		(0.074)	(0.077)
Staurastrum		0.105*	0.083		0.109	0.098
		(0.060)	(0.063)		(0.073)	(0.080)
Isomorphic Group		-0.020	-0.025		-0.096	-0.023
		(0.070)	(0.072)		(0.153)	(0.120)
Time Trend First Batch			-0.001***			-0.001**
			(0.000)			(0.000)
Time Trend Second Batch			0.000***			0.001**
			(0.000)			(0.000)
Selection Effect				-0.000	-0.000	0.000
				(0.000)	(0.000)	(0.000)
Complementarity Effect				-0.000	-0.000	0.000
				(0.000)	(0.000)	(0.000)
Constant	0.679	1.370	18.163***	24.846***	-3.518	16.972**
	(6.390)	(6.834)	(6.666)	(0.074)	(9.190)	(8.320)
R^2	0.204	0.246	0.400	0.009	0.312	0.432
N	169	169	169	129	129	129

Table S13. Regression results: mean RGB and T_{max} (quadratic).

Notes: $*p < 0.1, **p < 0.05, ***p < 0.01$. Robust standard errors in parentheses.

Dependent Variable: Temperature Maximum (°C)

	(1)	(2)	(3)	(4)	(5)	(6)
(RGB Mean)	0.342***	0.327***	0.087		0.407***	0.105
	(0.095)	(0.102)	(0.096)		(0.139)	(0.123)
(RGB Mean)^2	-0.001***	-0.001***	-0.000		-0.001***	-0.000
	(0.000)	(0.000)	(0.000)		(0.001)	(0.000)
Ankistrodesmus		-0.024	-0.109*		-0.057	-0.098
		(0.063)	(0.056)		(0.079)	(0.072)
Cosmarium		-0.042	-0.052		-0.053	-0.049
		(0.064)	(0.059)		(0.075)	(0.071)
Selenastrum		0.145**	0.095		0.124*	0.103
		(0.066)	(0.064)		(0.074)	(0.077)
Staurastrum		0.096	0.067		0.096	0.074
		(0.061)	(0.063)		(0.075)	(0.080)
Isomorphic Group		-0.016	-0.028		-0.084	-0.032
		(0.072)	(0.069)		(0.160)	(0.133)
Time Trend First Batch			-0.001***			-0.001**
			(0.000)			(0.000)
Time Trend Second Batch			0.001***			0.001***
			(0.000)			(0.000)
Selection Effect				-0.000	-0.000	0.000
				(0.000)	(0.000)	(0.000)
Complementarity Effect				-0.000	-0.000	0.000
				(0.000)	(0.000)	(0.000)
Constant	0.566	1.444	19.194***	25.162***	-3.894	17.871**
	(6.437)	(6.930)	(6.513)	(0.076)	(9.294)	(8.286)
R^2	0.227	0.264	0.430	0.010	0.324	0.451
N	169	169	169	129	129	129

Table S14. Regression results: mean RGB and T_{min} (quadratic).

Notes: $*p < 0.1, **p < 0.05, ***p < 0.01$. Robust standard errors in parentheses.

Dependent Variable: Temperature Minimum (°C)

	(1)	(2)	(3)	(4)	(5)	(6)
(RGB Mean)	0.295***	0.287***	0.085		0.331**	0.078
	(0.090)	(0.097)	(0.097)		(0.135)	(0.124)
(RGB Mean)^2	-0.001***	-0.001***	-0.000		-0.001**	-0.000
	(0.000)	(0.000)	(0.000)		(0.001)	(0.000)
Ankistrodesmus		-0.011	-0.079		-0.036	-0.070
		(0.060)	(0.055)		(0.074)	(0.070)
Cosmarium		-0.057	-0.058		-0.072	-0.061
		(0.061)	(0.058)		(0.071)	(0.070)
Selenastrum		0.127**	0.096		0.119*	0.109
		(0.063)	(0.064)		(0.070)	(0.076)
Staurastrum		0.094	0.079		0.096	0.085
		(0.059)	(0.062)		(0.071)	(0.078)
Isomorphic Group		-0.026	-0.024		-0.096	-0.035
		(0.068)	(0.072)		(0.145)	(0.116)
Time Trend First Batch			-0.001***			-0.001*
			(0.000)			(0.000)
Time Trend Second Batch			0.000**			0.000**
			(0.000)			(0.000)
Selection Effect				-0.000	-0.000	0.000
				(0.000)	(0.000)	(0.000)
Complementarity Effect				-0.000	-0.000	0.000
				(0.000)	(0.000)	(0.000)
Constant	3.506	3.914	18.766***	24.585***	0.909	19.177**
	(6.089)	(6.546)	(6.591)	(0.071)	(9.024)	(8.332)
R^2	0.178	0.216	0.349	0.008	0.277	0.384
N	169	169	169	129	129	129